

Electronic structure of double-gyroid nanostructured semiconductors: Perspectives for carrier multiplication solar cells

Sergei Khlebnikov^{1,2,*} and Hugh W. Hillhouse^{2,3,†}¹*Department of Physics, Purdue University, West Lafayette, Indiana 47907, USA*²*The Energy Center, Purdue University, West Lafayette, Indiana 47907, USA*³*School of Chemical Engineering, Purdue University, West Lafayette, Indiana 47907, USA*

(Received 27 April 2009; revised manuscript received 30 June 2009; published 16 September 2009)

A double-gyroid nanostructure is a two-component heterostructure that is three-dimensionally periodic, with one material forming a continuous wall-like region of nearly constant thickness centered on the zero-mean curvature G surface. The other material forms two individually continuous channel-like regions. Semiconductor nanostructures with this topology may now be fabricated, and we present here the first calculation of the electronic structure of such materials. We use the simplest two-band envelope function method that can yield information on the nature of quantum confinement effects. We report the density of states and wave functions for the case of PbSe and show that when PbSe fills the channel-like region, the resulting double-gyroid PbSe nanowire network displays quantum confinement effects with a blueshifted band gap of 0.50 eV (1.77 times the bulk PbSe band gap of 0.28 eV). In addition, the low-energy density of states (DOS) contains a series of peaks separated by gaps; we attribute the enhancement of the DOS in the peaks to a weak dependence of energy on the quasimomentum. Thus, we suggest that these structures may have some similarity with zero-dimensional or one-dimensional materials in regard to their photophysics, yet may have more similarity to three-dimensional materials with regard to their transport properties. As a result, they may be of aid in harnessing nonlinear optical effects, such as carrier multiplication phenomena, for high-efficiency photovoltaic or photoelectrochemical devices.

DOI: [10.1103/PhysRevB.80.115316](https://doi.org/10.1103/PhysRevB.80.115316)

PACS number(s): 73.21.Hb

I. INTRODUCTION

The phenomenon of “multiple exciton generation” (MEG) or “carrier multiplication” (CM) has been observed experimentally^{1,2} in semiconducting quantum dots with high efficiency using photons of visible wavelengths. This makes these systems potentially promising photoabsorbers in next generation photovoltaic or photoelectrochemical cells. However, harvesting the “extra” photogenerated electrons and holes from zero-dimensional (0D) quantum dots to yield a higher photocurrent is difficult and has yet to be shown experimentally. For a recent review of efforts to utilize quantum dots in solar cells see Ref. 3. In that critique a challenge was articulated to develop materials and devices that behave similar to 0D quantum confined objects in regards to their photophysics but behave more similar to 3D objects in regards to their electronic transport. One approach to this challenge is to assemble quantum dots into a three-dimensional (3D) array such that charge carriers can be extracted via tunneling between the dots. Another, which we consider here, is to use unique semiconductor nanostructures that are composed, effectively, of short one-dimensional (1D) nanorods that branch periodically so as to create a periodic 3D material composed of small aspect ratio cylindrical segments. This may provide a route to utilize 0D or 1D quantum phenomena in the photoexcitation process and still extract the enhanced photocurrent in a next generation solar cell.

The precise conditions for MEG to occur are at present not completely understood and are a topic of recent debate.^{4,5} However, we expect that, regardless of the precise mechanism, the electronic density of states (DOS) is important in determining the probability of MEG. Indeed, an enhance-

ment of the DOS aids single-exciton production, as the probability is directly proportional to the DOS. We expect it to play an even greater role in nonlinear effects (by which we mean effects involving a coupling between single-exciton and multiexciton states), where within perturbation theory there is a factor of DOS corresponding to each of the produced carriers.

Due to the presence of the branch points, the individual wire segments have finite lengths, which suggests that they may behave more like a collection of weakly coupled quantum dots or quantum rods, as opposed to an infinite length homogeneous quantum wire. Consider, for example, a wire-like structure formed by a weakly coupled periodic chain of resonance cavities. Within the tight-binding approximation, the spectrum of waves in such a wire has the form $E(q) - E(0) \propto 1 - \cos q$, where q is the quasimomentum. The DOS exhibits characteristic “horns” at $q=0, \pi$.

The question we address here is whether this enhancement mechanism may exist in new semiconductor nanostructures that may now be fabricated. Recently, Urade *et al.*⁶ reported the fabrication of continuous nanoporous silica thin films with the double-gyroid (DG) structure (see Fig. 1) and demonstrated their use in a template-replication nanofabrication technique by filling the pores with a metal and removing the original silica nanostructure. The result is a three-dimensionally periodic array of two interpenetrating metallic nanowire networks with a unit cell of approximately 18 nm. Each nanowire network can be viewed as a collection of nanowire segments (approximately cylindrical nanorods that are roughly 4 nm in diameter and 10 nm in length) joined at “y junctions” [Fig. 1(c)]. These junctions are oriented in space such that the nanostructure is three-dimensionally pe-

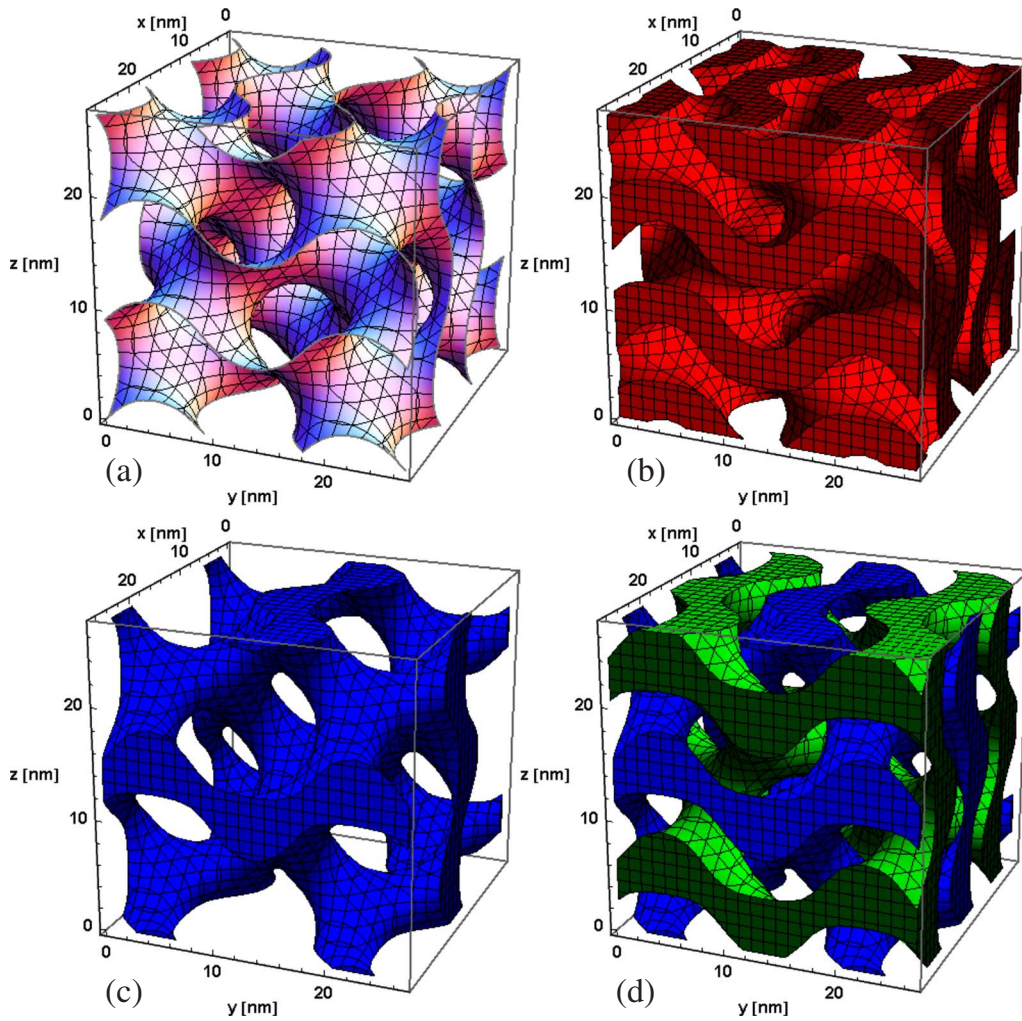


FIG. 1. (Color online) The double-gyroid structure with cubic symmetry (space group $Ia\bar{3}d$) and lattice constant $a=17.9$ nm. Each panel shows a region that is $1.5a$ to better illustrate the periodicity. (a) The G surface within the level-surface approximation of Ref. 7 (contour level 0). This surface defines two separate nonintersecting pore systems. (b) The double-gyroid structure that results when the infinitely thin G surface is replaced by a finite-thickness wall defined by contour levels -0.8 and 0.8 . (c) One of the nanowire networks that result from filling the pores of the double-gyroid structure. (d) Both of the interpenetrating, but nonintersecting, nanowire networks.

riodic with cubic $Ia\bar{3}d$ symmetry, giving a 3D character to the collection of nanowire segments. One can envision similar structures where the nanowire network is a semiconductor, rather than a metal, and the silica wall is either left in place or removed. Such materials could potentially be used to address the 0D photophysics–3D transport challenge discussed above and could potentially yield solar energy conversion devices that utilize MEG.

In these semiconductor nanostructures, either the junctions or the nanorods could in principle function as weakly coupled resonance cavities. Our goal was to find out if interference of electron waves in a double-gyroid nanostructured semiconductor is strong enough for either of those regions to actually behave in that way. We have chosen PbSe as the semiconductor to be used for the simulations since MEG has been observed in PbSe quantum dots.^{1,2} In addition, the near equality of the electron and hole effective masses in this material suggests that the DOS may be studied using an approximation involving relatively few parameters. Our strat-

egy has been to extract these parameters by fitting the experimentally measured absorption spectra of the spherical PbSe quantum dots² and then use the extracted values to numerically compute the spectrum of DG.

Here, we present results on the DOS and the shape of wave functions of semiconductor DG nanostructures. These results were obtained by numerically solving the scalar wave equation

$$[-c^2\nabla^2 + E_0^2(\mathbf{r})]\psi(\mathbf{r}) = E^2\psi(\mathbf{r}), \quad (1)$$

where $E_0(\mathbf{r})$ is half of the bulk band gap, which has different values in different spatial regions, and E^2 are the eigenvalues to be determined. Equation (1) is the simplest one containing two effects of main interest to us in the present study: the presence of a band gap and (via the ∇^2 term) of spatial dispersion. It can be viewed as a two-band (conduction and valence) version of the isotropic envelope approximation, often used in description of lead salt quantum dots.⁸ Thus, a state with $E > 0$ describes an electron, and a state with E

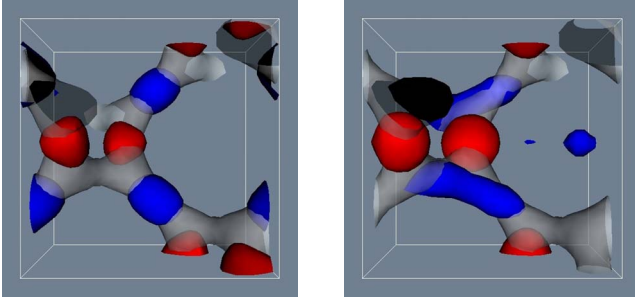


FIG. 2. (Color online) Hot spots in a double gyroid. Isosurfaces of the probability densities for states with $\mathbf{q}=0$, $n=19$ (left panel) and $\mathbf{q}=(\pi/a, 0, 0)$, $n=18$ (right panel). The “beads” are color coded to reflect the signs of the wave functions. The transparent white surface is an isosurface of the probability density in the ground state of the channel and is used to indicate the channel’s location.

< 0 a hole. Since the spectrum is symmetric with respect to $E=0$, in what follows we concentrate on the electron states. Extension to the full four-band formalism of Kang and Wise⁸ would significantly increase the size of the numerical problem and has been deferred to future work.

A spherical PbSe quantum dot with Dirichlet boundary conditions at $r=R$ corresponds to $E_0(r<R)=0.14$ eV and $E_0(r>R)=\infty$. In that case, Eq. (1) can be solved analytically. By fitting the dot absorption spectra, we find $c=0.28$ eV nm.

For a DG nanostructure, we assign different values of $E_0(\mathbf{r})$ to the materials in the wall and in the channels. We keep the same form of the equation (and indeed, here, the same value of c) for regions with both low and high band gaps. We expect this to be a good approximation whenever the ratio of the band gaps is sufficiently large to effectively confine the carriers to the low-band-gap region. As far as we know, this problem does not have an analytic solution. In addition to the case when a low-band-gap semiconductor fills the double-gyroid channels [hereafter referred to as the DG-wire case and shown in Fig. 1(d)], we have considered the inverted case, in which the semiconductor composes the wall itself. This geometry is the DG topology version of a two-dimensional quantum well and is hereafter referred to as the DG-well case [shown in Fig. 1(b)]. For this case, the assignment of the values of E_0 to the wall and channels has been reversed.

We have found that, in the DG-wire case, the low-energy DOS contains a series of peaks separated by gaps. Due to the high symmetry of the double-gyroid structure, some level degeneracies are present, but the peaks survive even after these degeneracies have been removed. A particularly large enhancement of DOS occurs for a group of states in which the wave functions are supported mostly in the cylindrical segments (see Fig. 2). This enhancement can be traced to an exceptionally weak dependence of energy on the quasimomentum.

The DG-well case bears some similarity to the case where a *metal* is confined to an (infinitely thin) gyroid *surface*, which was considered by Koshino and Aoki⁹ (see also Ref. 10). These authors have identified several peaks in the DOS and related them to the symmetries of the gyroid surface.

Here, we consider a finite-thickness semiconductor, rather than an infinitely thin metal. Moreover, our numerical method is designed for three-dimensional calculations—it samples the volume rather than a surface, so the limit of an infinitely thin wall is not accessible. Still, one expects that symmetry-related considerations should not be overly sensitive to the wall thickness, and indeed the level degeneracies reported for the infinitely thin metal⁹ are readily identified in our data. Upon removal of the degeneracies, the DOS in the DG-well case does not exhibit any peaks of strength comparable to that in the DG-wire case. This is consistent with the finding of Koshino and Aoki⁹ that the DOS can be smoothed out by adding a symmetry-breaking potential.

II. COMPUTATIONAL METHOD

We now turn to a more detailed description of our computations and results. The double-gyroid is a body-center cubic (bcc) structure with space group $Ia\bar{3}d$. The fabricated double-gyroid nanostructure thin films deviate from perfect cubic symmetry, as they contract more in one direction (perpendicular to the substrate) than in the other two.⁶ For an initial theoretical study, however, it is natural to start from the system with maximal symmetry. So, here, we present results for an uncontracted double-gyroid with cubic lattice constant $a=17.9$ nm. We have verified that, while the asymmetric contraction smears out the DOS in the DG-wire case, pronounced peaks remain.

Computationally, it is sufficient to consider a single unit cell. Given that the conventional double-gyroid unit cell is bcc, the corresponding primitive unit cell is rhombohedral and is formed by vectors drawn from the corner of the bcc cell to the body centers of three adjacent bcc cells. On the other hand, mathematical description of the DG structure and imposing the boundary conditions are simplified if one uses a cube with dimensions of a single bcc unit cell. Here, we adapt the latter approach, even though it is less computationally efficient since the cubic unit cell that we simulate has twice the volume of the primitive rhombohedral cell. Accordingly, the first Brillouin zone (BZ) spanned by quasimomenta \mathbf{q} of Eq. (2) is a simple-cubic BZ, with half the volume (in the reciprocal space) of the BZ that results from using the primitive unit cell. We discuss the relation between the two Brillouin zones in more detail later. (Let us stress that the BZ we are talking about is the BZ of the double-gyroid nanostructure, not that of the underlying PbSe crystal.) Thus, the periodic boundary conditions are imposed at the surface of the unit cube and have the form

$$\psi(\mathbf{r} + \mathbf{a}) = e^{i\mathbf{q}\cdot\mathbf{a}} \psi(\mathbf{r}), \quad (2)$$

where \mathbf{a} is a lattice translation and $\mathbf{q}=(q_x, q_y, q_z)$ is a quasimomentum.

In order to specify the values of $E_0(\mathbf{r})$ in the unit cell, a mathematical description of the double-gyroid is needed. While the gyroid surface is exactly represented by a Weierstrass-Enneper representation, the double-gyroid structure, where the wall has finite thickness, is more conveniently (and very accurately) represented by a level-surface approximation.⁷ Namely, the two wall-channel interfaces are

approximated by the equations $F(\mathbf{r}) = \pm w$, where

$$F(x, y, z) = \sin(2\pi x/a)\cos(2\pi y/a) + \sin(2\pi y/a)\cos(2\pi z/a) \\ + \sin(2\pi z/a)\cos(2\pi x/a),$$

and $0 \leq w \leq \sqrt{2}$ is a parameter determining the wall thickness ($w=0$ corresponding to an infinitely thin wall). The results below are for $w=0.8$, when the thickness of the wall and the transverse size of the channels are comparable.

For the parameters appearing in Eq. (1), we have used $c=0.28$ eV nm and, in the DG-wire case,

$$E_0(\mathbf{r}) = \begin{cases} E_l, & |F(\mathbf{r})| > w \text{ (channels)} \\ E_h, & |F(\mathbf{r})| < w \text{ (wall)}, \end{cases} \quad (3)$$

with the low energy $E_l=0.14$ eV (half of the bulk band gap of PbSe) and the high energy $E_h \approx 5.2$ eV. In the DG-well case, the energy assignments have been reversed. The large difference between E_l and E_h means that, as far as the low-energy spectrum is concerned, the wave function is confined to either the channels (the DG-wire case) or the wall (the DG-well case), with essentially zero boundary conditions at the interfaces.

In what follows, we often use dimensionless units in which energies are reported in units of half the bulk band gap of the semiconductor (E_l) and lengths in units of c/E_l . Thus, for the aforementioned values of the parameters, the unit of length equals 2 nm.

We have discretized Eq. (1) with the boundary condition (2) on a uniform spatial lattice and diagonalized the resulting matrix numerically using a general purpose routine.¹¹ Here, we present results from a 20^3 lattice; the corresponding matrix problem thus involves a 8000×8000 unitary matrix for each value of \mathbf{q} . By comparing the results to those from a 16^3 lattice, we have confirmed that there is enough spatial resolution to accurately reproduce the low-energy spectrum, on which our conclusions are based.

For each \mathbf{q} , the spectrum typically contains well-defined groups of degenerate states. These degeneracies may enhance the density of states at certain values of the energy. Such an enhancement is of interest in its own right but is not directly related to the strength of the coupling between neighboring cells of the three-dimensional material (i.e., the question of the existence of “hot spots,” which we primarily wish to explore). Therefore, in addition to the full DOS, we construct the quantity we call the reduced DOS (RDOS), in which the degeneracies have been removed. This is done by counting all states corresponding to the same \mathbf{q} and separated in energy by less than $\epsilon=10^{-4}E_l$ as one state. An enhancement in the RDOS will be due to similarity of energies corresponding to *different* values of the quasimomentum and thus a reflection of weak coupling between the segments or junctions.

III. RESULTS

We begin with the DG-wire case (semiconductor filling the channels). In Fig. 3, we show both the RDOS and the full DOS. In this case, their overall shapes are quite similar. In particular, moderately excited states (0.29 eV $< E$

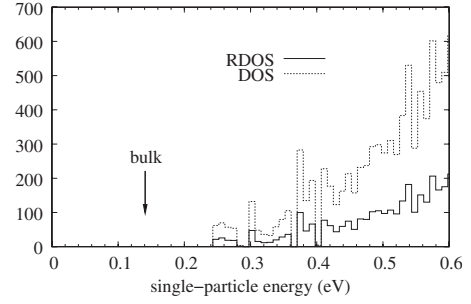


FIG. 3. Histograms of the reduced and full densities of single-particle (electron or hole) states for the case when PbSe (with bulk band gap of 0.28 eV) fills the channels of the double gyroid.

≤ 0.40 eV) form a number of sharp peaks separated by gaps. We also note that the band gap is quite blueshifted (equal to 1.77 times the bulk band gap)—a consequence of quantum confinement in the channels.

We interpret these peaks (enhanced RDOS) as a sign of weak coupling between neighboring unit cells. To confirm this interpretation, we have considered the nature of the wave functions corresponding to the peak at $E=0.3$ eV. In Fig. 2, we show isosurfaces of the probability densities of state number $n=19$ at $\mathbf{q}=0$ and state number $n=18$ at $\mathbf{q}=(\pi/a, 0, 0)$.¹² (The difference in the quantum number is inessential since each state is a member of a degenerate group of four with n ranging from 16 to 19.) Each isosurface is seen to be a collection of “beads” residing at the cylindrical segments that connect the y junctions. Either state is supported primarily in one of the two complementary nanowire networks.

One readily identifies common elements of the two wave functions in Fig. 2. The main difference between the two is that in the $\mathbf{q}=0$ state the sign of the wave function (represented by the color of the beads) always alternates between neighboring beads. In the $\mathbf{q} \neq 0$ state, the π twist in the x direction (which runs horizontally in the figure) pushes beads of the same color together, to form a single antinode. The energy difference between the two states (i.e., the bandwidth for waves propagating in the x direction), however, is small: $E(\pi/a) - E(0) = 1.7 \times 10^{-3} E_l = 0.23$ meV.

The profile of the wave function along the x direction in the presence of a π twist (a single antinode in the middle and vanishing wave function at the ends) suggests that a relevant “control” for comparison is a straight wire with band gap equal to the value of $E(0)$ above [$E(0)=0.3$ eV] and wave function twisted by π (antiperiodic boundary conditions) over a length $L=10=20$ nm. The twist supplies wave number π/L and energy

$$E(\pi/L) - E(0) \approx \frac{\pi^2 c^2}{2L^2 E(0)} = 3.2 \text{ meV}, \quad (4)$$

which is more than an order of magnitude larger than the energy difference between the states of Fig. 2. This quantifies how weakly coupled the neighboring cells of the double gyroid are.

The use of twisted boundary conditions to make conclusions about coupling between spatially separated regions is

somewhat reminiscent of the Edwards-Thouless¹³ approach to electron localization. The main difference, of course, is that we are not dealing with disorder; so our wave functions are still delocalized (Bloch) states. In view of the concordant use of boundary conditions, however, we will refer to delocalized states with exceptionally weak dependence of energy on the quasimomentum as *quasilocalized*.

We should remark, though, that the evidence for weak coupling presented above has been obtained only for relatively high excited states ($n=16, \dots, 19$ in the above example) and does not extend to the lowest-energy states forming the broad peak around $E=0.26$ eV (see Fig. 3). We now briefly discuss the nature of those states.

Because of the large band gap in the wall, the excitations practically do not tunnel between the channels, so there are two degenerate ground states, one per channel. (One of these ground states is shown by the transparent white surface in Fig. 2.) The lowest-excited states at $\mathbf{q}=0$ form a degenerate group of six and are supported primarily in the y junctions. The energy difference between these states and the corresponding group (of four states) at $\mathbf{q}=(\pi/a, 0, 0)$ is $0.018E_f$. This is only marginally smaller than the energy separation (4) in the straight wire. Hence, we find no evidence of 0D behavior for states with $E < 2E_f$.

Next, we turn to the case where the wall is the low-band-gap semiconductor and the channels are filled with an insulator (DG-well case). Here, we expect to find some correspondence with the results of Ref. 9 (for a metal on a gyroid surface). In Ref. 9, the band structure was mapped onto the BZ of a body-centered structure as described by a rhombohedral primitive unit cell (referred to here as the body-centered BZ). However, our boundary conditions (2) imply the BZ of a simple-cubic structure with the dimensions of the original body-centered unit cell, and we refer to that BZ as the simple-cubic BZ. The body-centered BZ has twice the volume of the simple-cubic BZ. Hence, states corresponding to quasimomenta not present in the simple-cubic BZ are aliased there, producing additional bands. For instance, the H point¹⁴ of the body-centered BZ maps into the zone center (Γ point) of the simple-cubic BZ, so the sixfold degeneracy at the H point found in Ref. 9 should show up as a group of six states at $\mathbf{q}=0$, above the ground state. These states are readily identified in our data. The P point of the body-centered BZ maps to the corner of the simple-cubic BZ, i.e., to $\mathbf{q}=(\pi/a, \pi/a, \pi/a)$. Reference 9 reports fourfold degeneracies for states at the P point. There are two inequivalent P points in the body-centered BZ but only one corner in the simple-cubic one. So, we may expect that, in our case, states at the BZ corner should come in groups of eight, and indeed they do.

The DOS and RDOS for the DG-well case are shown in Fig. 4. We see that the low-energy DOS is comparatively smooth and becomes even more so upon the removal of the degeneracies. Comparison of energies for different values of \mathbf{q} confirms that tight-binding effects, if any, are much weaker than in the DG-wire case.

IV. CONCLUSION

To summarize, we have presented numerical evidence that scalar waves described by Eq. (1) undergo enough interfer-

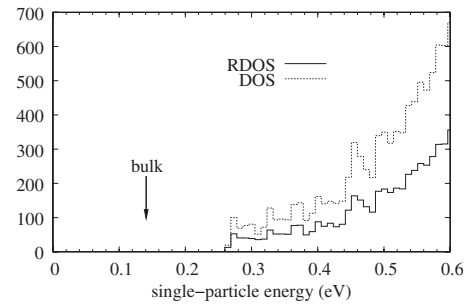


FIG. 4. Same as in Fig. 3 but for the case when PbSe fills the wall.

ence in double-gyroid semiconductor nanowire arrays to form “hot spots”—regions of localized excitation relatively weakly coupled to each other. The effect is especially strong for a group of excited states whose wave functions are supported primarily in the cylindrical segments connecting the y junctions (see Fig. 2).

On the other hand, the wave function corresponding to the band edge (the ground state) of a DG wire is completely delocalized. This suggests one way how photophysics may be separated from transport: carriers will be produced in the “hot spots,” relax to the band edge, and then be transported away. Such dynamics would go a long way toward realizing materials that are low dimensional in regard to their photophysics but three dimensional in regard to transport. Note that this scenario is quite different from what one expects for an array of quantum dots. If the QD array is a hexagonal close packing of QDs, then each QD has 12 nearest neighbors. Once the QDs are close enough to each other for the ground-state wave function to be completely delocalized, the material will likely behave like a bulk material in all respects.

The linear Eq. (1) does not include any interactions among the carriers and so does not allow one to directly assess the probability of carrier multiplication in a DG wire. We can, however, use an indirect method, based on estimating the time scale of charge transport between the “hot spots.” The bandwidth of 0.2 meV found above corresponds to transport time of a few picoseconds. This seems long enough for MEG in the cylindrical segments to take place essentially in the same way as it does in quantum dots (where, according to Ref. 15, it proceeds at the subpicosecond scale). Thus, we suggest that the blueshift in the band gap, the enhanced density of states, and the existence of quasilocalized wave functions in semiconducting wires based on double-gyroid nanostructures may make them of use for MEG based solar cells and other optical processes where interactions between single-exciton and multiexciton states are important. However, since at present there is no agreed upon theory of MEG, even in the well-studied case of PbSe quantum dots, evaluation of this possibility will require further theoretical, as well as experimental, efforts. In particular, we believe that ultrafast spectroscopy experiments in the form of transient absorption or time-resolved photoluminescence would be particularly informative.

*skhle@physics.purdue.edu

†hugh@purdue.edu

- ¹R. D. Schaller and V. I. Klimov, Phys. Rev. Lett. **92**, 186601 (2004).
- ²R. J. Ellingson, M. C. Beard, J. C. Johnson, P. Yu, O. I. Micic, A. J. Nozik, A. Shabaev, and A. L. Efros, Nano Lett. **5**, 865 (2005).
- ³H. W. Hillhouse and M. C. Beard, Curr. Opin. Colloid Interface Sci. **14**, 245 (2009).
- ⁴A. J. Nozik, Chem. Phys. Lett. **457**, 3 (2008).
- ⁵O. V. Prezhdo, Chem. Phys. Lett. **460**, 1 (2008).
- ⁶V. N. Urade, T.-C. Wei, M. P. Tate, J. D. Kowalski, and H. W. Hillhouse, Chem. Mater. **19**, 768 (2007).
- ⁷M. Wohlgemuth, N. Yufa, J. Hoffman, and E. L. Thomas, Macromolecules **34**, 6083 (2001).
- ⁸I. Kang and F. W. Wise, J. Opt. Soc. Am. B **14**, 1632 (1997).
- ⁹M. Koshino and H. Aoki, Phys. Rev. B **71**, 073405 (2005).
- ¹⁰N. Fujita and O. Terasaki, Phys. Rev. B **72**, 085459 (2005).
- ¹¹We have used routines from the CLAPACK library (see <http://www.netlib.org/clapack>).
- ¹²Visualization of the probability density was done using the Visualization ToolKit (VTK) by Kitware, Inc. (<http://www.vtk.org>).
- ¹³J. T. Edwards and D. J. Thouless, J. Phys. C **5**, 807 (1972).
- ¹⁴For naming of special points in the body-centered cubic BZ, see, for example, V. Heine, *Group Theory in Quantum Mechanics* (Pergamon Press, New York, 1960).
- ¹⁵R. D. Schaller, V. M. Agranovich, and V. I. Klimov, Nat. Phys. **1**, 189 (2005).